The Canadian Mineralogist
Vol. 43, pp. 1589-1603 (2005)

CHEMICAL STATE OF SULFUR IN NATURAL AND SYNTHETIC LAZURITE BY S *K*-EDGE XANES AND X-RAY PHOTOELECTRON SPECTROSCOPY

MICHAEL E. FLEET[§], XIAOYANG LIU, SARAH L. HARMER[¶] AND H. WAYNE NESBITT[§]

Department of Earth Sciences, University of Western Ontario, London, Ontario N6A 5B7, Canada

ABSTRACT

Lazurite with a composition close to $[Na_6Ca_2Al_6Si_6O_{24}(SO_4,S)_2]$ has been synthesized by employing CaS + $CaSO_4$ redox in hydrothermal-pressure experiments and reduction with Re foil in piston–cylinder experiments. A royal blue lazurite formed by annealing at 1200°C and 0.5 GPa; it has an Al-rich framework (Al/Si between 1.1 and 1.2) and coexists with minor amounts of a colorless sodalite phase of S-poor, Si-excess composition. The sodalite phase of experiments without a reducing agent is haüyne. The chemical state of sulfur in the synthetic products and in lazurite from Afghanistan and Baffin Island, Nunavut, has been investigated by S *K*-edge X-ray absorption near-edge structure (XANES) spectroscopy and S 2*p* X-ray photoelectron spectroscopy (XPS). Sulfate is the dominant species of sulfur in all samples of lazurite studied, and there are significant but subordinate amounts of sulfide bound only to Na^+ cations. In addition, there is minor sulfite in some piston–cylinder products and minor native sulfur in the minerals. Polysulfides are not present above minimum levels of detection. Natural lazurite differs markedly from its synthetic equivalent in chemical composition and S *K*-edge XANES and S $2p_{3/2}$ XPS spectra, but these differences appear to have little bearing on color development. In synthetic haüyne, the cage sulfur species is exclusively sulfate.

Keywords: lazurite, synthesis, X-ray absorption near-edge structure (XANES), X-ray photoelectron spectroscopy (XPS).

SOMMAIRE

Nous avons synthétisé la lazurite ayant une composition voisine de $[Na_6Ca_2Al_6Si_6O_{24}(SO_4,S)_2]$ en employant comme réactifs CaS + $CaSO_4$ dans des expériences hydrothermales sous pression et par réduction d'une feuille de Re dans des expériences avec piston–cylindre. Nous avons obtenu un échantillon bleu royal par recuit à 1200°C et 0.5 GPa; la trame de ce matériau est enrichie en Al (Al/Si entre 1.1 et 1.2), et il coexiste avec une petite quantité de sodalite incolore à faible teneur en soufre et contenant un excédant de Si. Le membre du groupe de la sodalite formé dans les expériences sans agent réducteur est la haüyne. Nous avons déterminé l'état du soufre dans les produits de synthèses et dans la lazurite de l'Afghanistan et l'île de Baffin, au Nunavut, par spectroscopie de l'absorption des rayons X près du seuil *K* du soufre (XANES) et par spectroscopie photo-électronique des rayons X du S 2*p* (XPS). C'est le sulfate qui prédomine parmi les espèces de soufre dans tous les échantillons de lazurite, et nous décelons des quantités importantes mais subordonnées de sulfure en coordinence avec les cations Na^+. De plus, il se trouve une fraction mineure de sulfite dans certains produits issus de l'appareil piston–cylindre, et de soufre natif dans les minéraux étudiés. Les polysulfures ne dépassent pas le seuil de détection. La lazurite naturelle diffère de façon marquée de son équivalent synthétique en termes de composition chimique et des spectres XANES du seuil *K* du soufre et XPS du soufre $2p_{3/2}$, mais ces différences ne semblent pas exercer une grande influence sur le développement de la couleur. Dans la haüyne synthétique, le soufre situé dans la cage structurale serait exclusivement sous forme de sulfate.

(Traduit par la Rédaction)

Most-clés: lazurite, synthèse, spectroscopie de l'absorption des rayons X près du seuil *K* du soufre (XANES), spectroscopie photo-électronique des rayons X du S 2*p* (XPS).

§ *E-mail addresses*: mfleet@uwo.ca, hwn@uwo.ca
¶ *Present address*: CSIRO Manufacturing and Infrastructure Technology, PO Box 4, Woodville, SA 5011, Australia. *E-mail address*: sarah.harmer@csiro.au

Introduction

Lazurite, a member of the sodalite group (Hassan *et al*. 1985, Gaines *et al*. 1997), is notable for its color (rich royal blue, azure, violet-purple, greenish blue; Fig. 1). Royal blue material from Sar-e-Sang, Badakhshan Province, Afghanistan, has been prized as a blue pigment from antiquity, when it was known as *ultramarinum*. Lazurite occurs in association with calcite, pyrite, diopside, humite, forsterite, haüyne (or sodalite) and muscovite in contact and regionally metamorphosed carbonate rocks; the bright blue-colored rock is known as *lapis lazuli*. The natural pigment is now rarely available, but sodalite-group phases with a wide range of colors controlled by chemistry and known as "*ultramarine*" are synthesized on a commercial scale, and have become important industrial pigments. Lazurite and the synthetic "ultramarine" pigments have exceptional thermal and chemical stability. They are, however, extremely susceptible to mineral acids (even in minute amounts or in diluted form) and acid vapors; for example, they are bleached by acetic acid and break down rapidly in the presence of mineral acids, with the evolution of H_2S.

In the present study, we synthesized royal blue lazurite, and investigated the *T*, *P* and compositional controls on stability (or formation) of lazurite and its solid solution with other members of the sodalite group. The chemical state and local environment of sulfur in natural and synthetic lazurite are probed using S *K*-edge X-ray absorption near-edge structure (XANES) spectroscopy and X-ray photoelectron spectroscopy (XPS). Preliminary S *K*-edge XANES study of blue and green lazurite from Baffin Island showed that sulfur is present dominantly as sulfate, with only subordinate amounts of reduced sulfur species (Cade 2003). Finally, lazurite samples from the Baikal region, Russia, have been investigated recently by XPS (Tauson & Sapozhnikov 2003); S^{6+} and S^{2-} were identified in light blue lazurite, S^{6+}, S_n and S in dark blue lazurite, and S^{6+} and S^{4+} in a dark blue sample bleached by annealing in air.

Background Information

Sodalite constitutes a group of aluminosilicate clathrate minerals with the general formula $A_8[T_{12}O_{24}]X_2$ (Barth 1932), where *T* represents framework cations and *A* and *X* represent cavity cations and anions, respectively. The four members of the mineral group crystallize in the cubic space-group $P\bar{4}3n$; their ideal end-member composition and unit-cell parameter, as given in Gaines *et al*. (1997) are: 1) sodalite: $Na_8Al_6Si_6O_{24}Cl_2$, *a* 8.882 Å; 2) nosean: $Na_8Al_6Si_6O_{24}(SO_4)\bullet H_2O$, *a* 9.084 Å; 3) haüyne: $Na_6Ca_2Al_6Si_6O_{24}(SO_4)_2$, *a* 9.116 Å; and 4) lazurite: $Na_6Ca_2Al_6Si_6O_{24}S_2$, *a* 8.882 Å. There are several other sodalite-structure minerals of different framework composition or more exotic chemical composition that are not presently included in the sodalite group. The framework of the sodalite group consists of alternating AlO_4 and SiO_4 tetrahedra that are corner-linked to give the characteristic cubo-octahedral cavity of the sodalite structure. Aluminum and Si are ordered, even in haüyne and nosean (Hassan & Grundy 1984, 1989, 1991, Hassan *et al*. 1985); in comparison, Fleet (1989) found incipient (12%) disorder of the framework cations in a synthetic aluminogermanate sodalite ($Na_8Al_6Ge_6O_{24}Cl_2$). Synthetic haüyne and nosean exhibit complete solid-solution at 600°C and 1000 bars $P(H_2O)$ (Peteghem & Burley 1963). There is extensive solid-solution in nature between haüyne and nosean, and more limited solution of these minerals with sodalite (Taylor 1967). In addition, Taylor

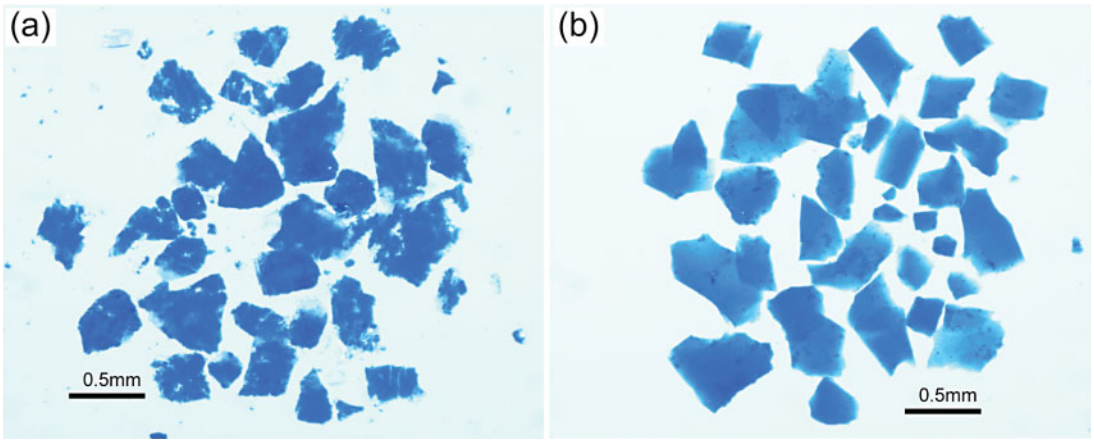

FIG. 1. (a) Deep royal blue lazurite from Afghanistan (2746), and (b) royal blue synthetic lazurite from experiment LZ67 (1200°C and 0.5 GPa): grains in nujol oil; overhead illumination.

(1967) emphasized the importance of K in haüyne and nosean; he showed that contents, in the range from 1 to 5 wt% K_2O, result in a progressive linear increase in the unit-cell edge. This high K_2O content no doubt reflects the high-temperature (volcanic) paragenesis of these two minerals.

Although the above ideal end-member compositions are in common usage, sodalite nomenclature is problematical, particularly for lazurite. Taylor (1967) did not discuss lazurite, but included material from the type locality within the composition field of haüyne. Belying the above ideal formula, mineral compositions of lazurite suggest that sulfate is much more important than reduced sulfur (*e.g.*, Hogarth & Griffin 1976). Thus, Strunz (1970) suggested the formula $(Na,Ca)_8Al_6Si_6O_{24}(SO_4,S,Cl)_2$, and other authors have included hydroxyl in the list of cavity anions as well. Also, the natural and synthetic samples of lazurite in this study all proved to be sulfate-dominant. On the other hand, haüyne of volcanic paragenesis does not seem to contain measurable amounts of reduced sulfur. Lazurite is further distinguished from haüyne by its intense color, which is commonly associated with the content of reduced sulfur. Therefore, for convenience in the present paper, natural and synthetic lazurite is defined within the sodalite group by (SO_4 + reduced S) = 1 to ~2 *pfu*, and haüyne by $SO_4 \leq 2$ *pfu*, reduced S $\approx$ 0; other synthetic materials having the sodalite structure with (SO_4 + reduced S) < 1, and lacking Cl and probably H_2O and OH also, are referred to as sodalite.

The aluminosilicate framework of sodalite allows a very wide range of cage cation and anion substituents; "ultramarine" compositions containing Na, S, Ag, Ag–Na, Tl, Sr, Ba, Zn, Mn, Pb, and Se were synthesized in early research (*e.g.*, Jaeger 1929). Commercial "ultramarine" pigments are generally based on a Na-reduced S end-member, with idealized formulae of the type $Na_8Al_6Si_6O_{24}S_4$ (Clark & Franks 1975), $Na_{6.9}Al_{5.6}Si_{6.4}O_{24}S_{2.0}$ (Reinen & Lindner 1999) or $Na_6Al_6Si_6O_{24}{\bullet}NaS_3$ (Gobeltz-Hautecoeur *et al*. 2002). It is generally accepted that the characteristic color of "ultramarine" is associated with the reduced sulfur (or chalcogen) content and, specifically, with the presence of the polysulfide S_3^- and S_2^- radical anion color centers (Clark & Franks 1975, Clark *et al*. 1983, Gobeltz *et al*. 1998a, b, Reinen & Lindner 1999, Gobeltz-Hautecoeur *et al*. 2002). Less than half of the sodalite cages are occupied by the S_3^- radical in typical "ultramarine" pigment (Gobeltz-Hautecoeur *et al*. 2002). Investigative methods have included electron paramagnetic resonance, Raman resonance and optical (electronic) spectroscopy. The polysulfide radical S_3^- is thought to be dominant in lazurite and blue "ultramarine" and, therefore, is assigned as the blue chromophore, whereas S_2^- alone imparts a yellow color, and more nearly equal amounts of the two chromophores give green. Partial substitution by Se results in pink to brown "ultramarine". Thus, by appropriate manipulation of chemical composition and preparation procedure, it is possible to make the spectrum of pigments from purple "ultramarine" to pink (or red) "ultramarine". Synthesis of "ultramarine" generally involves annealing a reactive aluminosilicate base, sulfur and a sodium compound in the presence of a reducing agent, usually followed by a final annealing stage at lower temperature in an oxidizing environment. For example, commercial "ultramarine" blue is made from a mixture of (anhydrous) metakaolin, S, Na_2CO_3, and a reducing agent (oil), heated in a controlled reducing atmosphere at about 750°C, and then in an oxidizing atmosphere at 450°C. The S_3^- radical starts to form at about 300°C by reaction of sulfide (S^{2-}) and sulfur, and its concentration increases with increase in temperature (Gobeltz *et al*. 1998b).

In related research, Clark *et al*. (1983) noted that the blue colour formed when alkali metal polysulfides are dissolved in donor solvents like dimethylformamide and hexamethylphosphoramide also is attributable to the S_3^- radical anion. Of greater significance for this study, and also discussed in Clark *et al*. (1983), small amounts of this chromophore are responsible for the deep blue color of sulfur dissolved in alkali chloride melts (*e.g.*, Berg & Bjerrum 1980). By quenching from the melt, it is possible to dope S_3^- and S_2^- isomorphically in very small amounts into the halogenide positions of alkali halides, bromides and iodides.

Experimental Methods

The synthesis of lazurite was investigated using sealed evacuated silica glass tube, hydrothermal bomb, and piston–cylinder techniques (Table 1). Starting compositions were prepared from analytical grade CaS, anhydrous $CaSO_4$, $CaSO_4{\bullet}2H_2O$, Na_2S, and native sulfur, and a base mixture of ideal nepheline composition ($NaAlSiO_4$; NAS), which was prepared by fritting a stoichiometric mixture of analytical grade Na_2CO_3, high-purity Al_2O_3 and amorphous SiO_2 in a platinum crucible at 1000°C for about 1 hour. For the single experiment in a sealed-silica-glass tube (LZ31), the starting mixture was contained in a welded platinum capsule within the evacuated tube, and the experiment was quenched in air and water. In the hydrothermal-pressure experiments, the starting mixture was contained in a welded gold capsule; batches of two to four capsules were reacted in a Tuttle bomb, which was quenched with water. High-pressure experiments were made in end-loaded piston–cylinder devices using 1.9 cm assemblies. All but two experiments (LZ21 and LZ22) used a Depths of the Earth Company Quickpress. For both the Quickpress and a second piston–cylinder apparatus, all furnace parts were previously fired at 1000°C in air. The NAS base, CaS and $CaSO_4$ were dried at 1000°C for 12 hours, and $CaSO_4{\bullet}2H_2O$ at 105°C for 12 hours. Pressure was calibrated from melting of dry NaCl at 1050°C (Bohlen 1984) and transformation of quartz to coesite at 500°C (Bohlen & Boettcher 1982). Temperature was

TABLE 1. EXPERIMENTS ON SYNTHESIS OF LAZURITE

Expt.	Starting composition[1] (molar proportions)	T (°C)	P (GPa)	Time (hours)	Assemblage[2] of products	Color	*a* (Å)
			Sealed silica-glass tube				
LZ31	6NAS+2CaS[3]	1200	<1 bar	0.5	Ne + Old	colorless	-
			Hydrothermal pressure				
LZ04	7NAS+6$CaSO_4$•2H_2O+9H_2O	890	0.14	0.1	Hgr + "Gl"	colorless	-
		890-570[4]	0.12	120			
LZ07	6NAS+CaS+$CaSO_4$	810	0.1	140	Lzr + Ne*	blue	9.074(3)
LZ08	6NAS+CaS+$CaSO_4$•2H_2O	810	0.1	140	Lzr + Gp + Ne[¶]	light grey	-
LZ09	6NAS+2CaS	805	0.1	140	Ne + Lzr*	dark grey	-
LZ10	6NAS+$CaSO_4$	805	0.1	140	Lzr + Ne[¶]	pale blue	-
LZ11	6NAS+2$CaSO_4$•2H_2O	805	0.1	140	Hyn	colorless	9.118(3)
LZ12	6NAS+2CaS+2S	805	0.1	140	Ne + Lzr	green	-
LZ13	6NAS+0.2CaS+1.8$CaSO_4$	795	0.1	140	Lzr + Ne*	royal blue	-
LZ14	6NAS+0.4CaS+1.6$CaSO_4$	795	0.1	140	Lzr + Ne	royal blue	-
LZ15	6NAS+0.6CaS+1.4$CaSO_4$	795	0.1	140	Ne + Lzr	light blue	-
LZ16	6NAS+0.8CaS+1.2$CaSO_4$	795	0.1	140	Ne + Lzr	bluish grey	-
LZ17	6NAS+1.2CaS+0.8$CaSO_4$	800	0.1	140	Ne + Lzr	grey-brown	-
			Piston cylinder				
LZ21	6NAS+2$CaSO_4$•2H_2O	1200	1.2	5	Gl	colorless	-
LZ22	6NAS+2$CaSO_4$	1100	1.5	24	Hyn	colorless	9.071(1)
LZ26	6NAS+2$CaSO_4$	1100	0.5	48	Hyn	colorless	9.0887(7)
LZ27	6NAS+2$CaSO_4$.2H_2O	1200	0.5	24	Hyn	colorless	9.095(1)
LZ28	6NAS+2$CaSO_4$	1400	0.5	0.5	Hyn + Gl*	colorless	9.093(1)
LZ29	6NAS+2CaS	1400	0.5	1	Gl	colorless	-
LZ30	6NAS+CaS+$CaSO_4$	1400	0.5	1	Gl	colorless	-
LZ62	6NAS+CaS+$CaSO_4$ (+Re)	1400	0.5	2	Lzr + ReS_2	royal blue	-
LZ65	6NAS+CaS+$CaSO_4$ (+Re)	1400	0.5	0.3	Lzr + ReS_2	royal blue	9.096(1)
		1200	0.5	15			
LZ66	6NAS+0.25CaS+1.75$CaSO_4$ (+Re)	1400	0.5	0.3	Lzr + ReS_2	grey	9.099(3)
		1200	0.5	15			
LZ67	6NAS+0.5CaS+1.5$CaSO_4$ (+Re)	1400	0.5	0.3	Lzr + ReS_2	deeper royal blue	9.089(3)
		1200	0.5	15			
BU01	6NAS+Na_2S+5S (+Re)	1400	0.5	0.3	Ne + ReS_2	colorless	-
		1200	0.5	14			
BU02	6NAS+Na_2S+5S (+Re)	850	0.5	48	"ultramarine" +Ne +ReS_2	blue	-

[1] NAS is $NaAlSiO_4$. Other symbols: Gp: gypsum, Hgr: hydrogrossular, Hyn: haüyne, Lzr: lazurite, Old: oldhamite (CaS).
[2] Lazurite is lazurite or related reduced-S-bearing sodalite; nepheline is nepheline or phase with a derivative nepheline structure.
[3] Contained in alumina crucible. [4] Cooling ramp.

measured by inserting a Pt–Pt90%Rh10% thermocouple into the high-pressure cell. The starting mixture was encapsulated in a sealed platinum tube with a diameter of 5 mm and a height of 12 mm, which was separated from a graphite tube by MgO powder; for experiments LZ62 to LZ67 and BU01 and BU02 (Table 1), the platinum capsule was lined on inside surfaces with Re metal foil. All experiments were quenched at pressure by switching off the furnace. Mineral samples were obtained from the Dana Mineral Collection at UWO. Lazurite 2746 is from an unknown location in Afghanistan; it was purchased in Germany from a mineral collector, and most likely is from the Sar-e-Sang locality. Lazurite 1343 is from Lake Harbour, Baffin Island, Nunavut (Hogarth & Griffin 1976, 1978, Cade 2003); scapolite 202 is from Tsarasaotra, Madagascar, and scapolite 1810 is from Craigmont, Ontario. The two samples of scapolite are monomineralic single crystals, and the two samples of lazurite were hand-separated to exclude contamination by pyrite, and to remove most of the calcite and Mg-silicate gangue.

Experimental products and minerals were characterized by optical microscopy, powder X-ray diffraction and electron-probe micro-analysis (EPMA; Figs. 1 to 3, Table 2). We used the JEOL JXA–8600 electron microprobe at UWO operated at 15 kV, 5 nA (measured

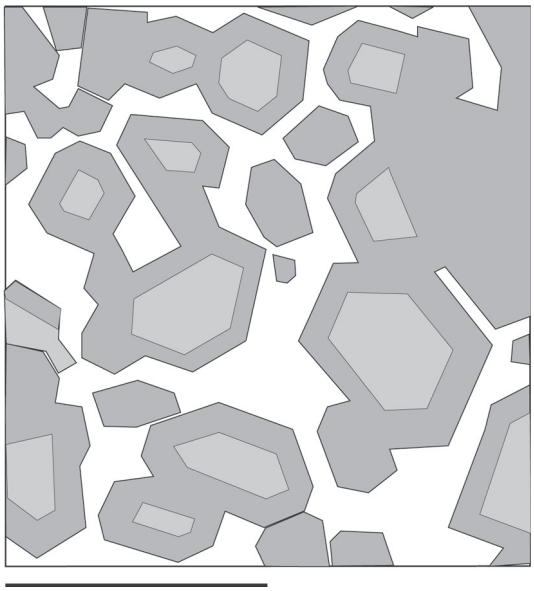

FIG. 2. Sketch of EPMA electron back-scattering image of royal blue lazurite from experiment LZ67: note that core-to-margin contrast of blue crystals of lazurite is exaggerated; scale bar is 10 μm.

on a Faraday cup), defocused beam, and mineral standards (albite for Na, Al and Si, Wakefield diopside for Ca and Mg, fayalite for Fe, orthoclase for K, anhydrite for S, and sodalite for Cl). For the experimental products, counting times were 20 s for all elements, and background measurements were made. For scapolite, the counting time for Na was reduced to 15 s, and for EPMA of natural lazurite, the background measurement for Na was switched off after the first spot, and counting times were 5 s for Na, which was measured first, 60 s for S and 20 s for other elements.

Sulfur *K*-edge XANES spectra were collected at the Canadian Synchrotron Radiation Facility (CSRF), Aladdin storage ring (University of Wisconsin at Madison, Wisconsin), using the double-crystal monochromator (DCM) beamline in both total electron yield (TEY) and fluorescence yield (FY) modes as a function of incident photon energy. Most samples were crushed, lightly ground and uniformly distributed on double-sided conducting carbon tape affixed to a clean stainless steel disk. One sample of LZ67 (Table 1) was in the form of a thin polycrystalline plate cleaved from the compacted experimental product. Other experimental details for the synchrotron radiation study are given in the accompanying paper (Fleet *et al*. 2005). For data reduction and analysis, we used the BAN and BGAUSS data-analysis programs (Tyliszcak 1992)

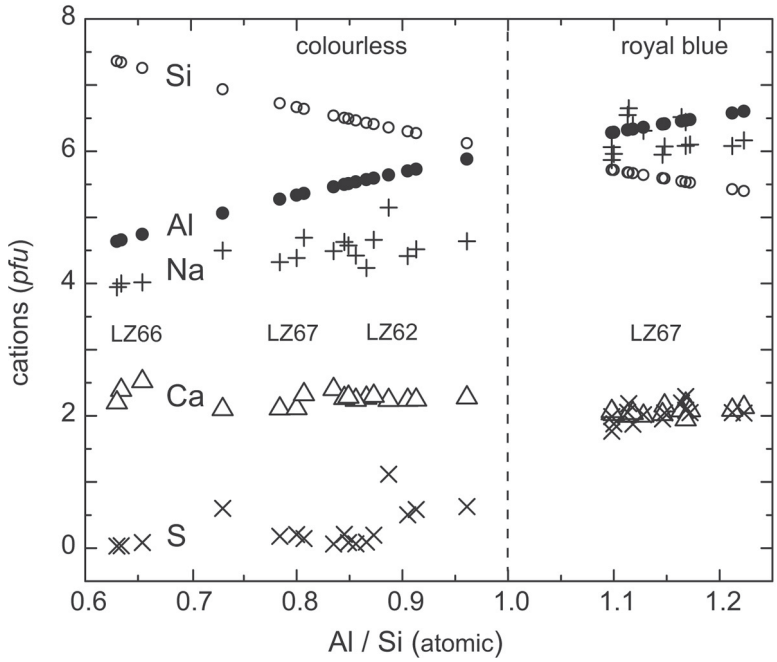

FIG. 3. EPMA spot compositions of synthetic royal blue lazurite from LZ67 and colorless matrix from this and other piston–cylinder experiments.

and FORTRAN77 codes, and the XANES spectra were normalized against incident intensity (I_o), which was measured simultaneously, and calibrated to the *K*-edge peak of native S at 2472.0 eV.

X-ray photoelectron spectroscopy (XPS) measurements used a Kratos Axis Ultra instrument fitted with a monochromated Al*K*α X-ray source (1487 eV) operated at 15 kV and 14 mA and a spot size of 300 μm. The detector was at normal incidence to the sample surface, enabling analysis to a depth of 50–100 Å. Samples were generally ground in a glove box filled with dry Ar gas and attached to the XPS spectrometer, prior to being evacuated in the reaction chamber at approximately 1×10^{-7} Torr; LZ67 was also prepared as a thin polycrystalline plate. The samples were then transferred into the analytical chamber, which was maintained at 2×10^{-9} Torr. Survey spectra were collected using a pass energy of 160 eV and a step size of 0.7 eV, to evaluate sample purity. High-resolution spectra were collected at 20 eV pass energy using a step size of 0.025 eV. The Kratos charge-neutralization system was used with a filament current of 1.6 A and a charge-balance voltage of 2.4 V, for the duration of each experiment. The spectrometer was standardized to the Au 4*f* line at 84.0 eV and calibrated using the Cu $2p_{3/2}$ line at 936.6 eV. The S 2*p* spectra show spin-orbit splitting, with the S $2p_{3/2}$ and S $2p_{1/2}$ lines separated by 1.19 eV and having relative peak-areas of 2:1 (*e.g.*, Nesbitt *et al.* 2000). Peak shapes of 50% Gaussian – 50% Lorentzian were used to fit the spectra, after subtraction of Shirley backgrounds (Shirley 1972).

TABLE 2. COMPOSITIONS OF LAZURITE AND SCAPOLITE

	Lazurite Afghanistan		Lazurite Baffin Island		Lazurite Synth.	Scapolite Madagascar	Scapolite Ontario
	2746	Taylor[1]	1343	H&G[1]	LZ67	202	1810
SiO_2 wt%	35.35	31.34	36.06	33.3	29.99	51.34	53.41
Al_2O_3	26.92	26.27	27.35	26.4	29.04	24.31	23.02
Fe_2O_3	-	0.27	-	0.00	-	-	-
FeO	0.02[2]	0.00	0.03[2]	0.00	-	0.05[2]	0.09[2]
MgO	0.03	2.47	0.02	0.00	-	0.02	0.00
CaO	6.30	7.97	6.05	5.3	10.27	12.13	9.05
Na_2O	18.51	15.75	18.89	18.8	17.16	6.60	8.43
K_2O	0.82	1.02	0.05	0.02	-	0.55	0.81
SO_3	15.62[3]	8.71	13.89[3]	10.91	14.50[3]	0.89[3]	1.10[3]
S	-	1.84	-	1.72	-	-	-
Cl	0.39	0.78	0.15	0.20	-	1.63	2.26
LOI	-	3.87	-	-	-	-	-
Subtotal	103.97	100.29	102.50	96.65	100.95	97.52	98.17
O≡Cl,S	0.09	1.10	0.03	0.91	0.00	0.37	0.51
Total	103.88	99.19	102.47	95.74	100.95	97.15[4]	97.66[4]
n	10	-	10	-	15	8	8
Si *apfu*	6.33	6.04	6.34	6.20	5.60	7.70	7.96
Al	5.67	5.96	5.66	5.80	6.40	4.30	4.04
Fe^{3+}	0.00	0.04	0.00	0.00	0.00	0.00	0.00
Fe^{2+}	0.00	0.00	0.01	0.00	0.00	0.01	0.01
Mg	0.01	0.71	0.01	0.00	0.00	0.00	0.00
Ca	1.21	1.65	1.14	1.06	2.06	1.95	1.44
Na	6.42	5.88	6.44	6.79	6.22	1.92	2.43
K	0.19	0.25	0.01	0.01	0.00	0.11	0.15
Total *A*	7.83	8.53	7.60	7.86	8.28	3.99	4.04
S^{6-}	1.23	1.26	1.29	1.53	1.81	0.10	0.12
S^{2-}	0.87	0.66	0.54	0.60	0.22	0.00	0.00
Cl	0.12	0.26	0.05	0.06	0.00	0.42	0.57
Total *X*	2.22	2.49	1.88	2.19	2.03	0.52[5]	0.69[5]

Compositions are recalculated on the basis of 12 (Si + Al) atoms per formula unit (*apfu*). [1] Taylor: Anal. 20 of Taylor (1967); H&G: anal. 6-1 of Hogarth & Griffin (1976). [2] total Fe as FeO. [3] total S as SO_3. [4] CO_2 not included. [5] CO_3 not included.

Results and Discussion

Synthesis of lazurite

A sodalite phase was formed in all experiments containing Ca-sulfate-bearing stoichiometric lazurite [$Na_6Ca_2Al_6Si_6O_{24}(SO_4,S)_2$] starting composition and run at 0.1 to 1.5 GPa from 795°C up to the temperature of melting (Table 1). The reaction to the sodalite phase was consistently complete for starting mixtures with sulfur added exclusively as Ca sulfate, whereas Ca sulfate + CaS tended to yield the assemblage lazurite + nepheline. On the other hand, a sodalite phase formed only sparingly with CaS as the only S-bearing reagent. It appears that lazurite of the ideal composition in the literature ($Na_6Ca_2Al_6Si_6O_{24}S_2$) has a limited field of stability in the pressure range presently investigated. Interestingly, the low-pressure experiment LZ31 yielded nepheline + CaS (Table 1), clearly demonstrating that the sulfur was not bound in a silicate phase. The sealed evacuated silica glass-tube technique was not used more extensively in this study owing to a lack of reaction at low temperature and the loss of volatile products at high temperature. Haüyne and lazurite are no doubt stable at low pressure and, indeed, we report in the accompanying paper (Fleet *et al.* 2005) that a sodalite phase precipitated on quenching a melt of $Na_6Ca_2Al_6Si_6O_{24}S_2$ composition in a sealed evacuated silica-glass tube experiment (LZ42).

The four piston–cylinder experiments with Re metal foil and Ca-bearing starting compositions (LZ62 to LZ67) yielded ReS_2 at the contact between the charge and Re foil. The Re foil was added in an attempt to suppress sulfidation of the platinum capsule by sulfur redox reactions in the charge; *e.g.*:

$$CaSO_4 + 3CaS = 2S_2 + 4CaO \quad (1)$$

Instead, ReS_2 formed, presumably by reaction of the type:

$$CaSO_4 + 3CaS + 2Re = 2ReS_2 + 4CaO \quad (2)$$

The rhenium sulfide contaminated the crushed silicate product of the first few experiments, but with appropriate care, it was found possible to remove the compact silicate plug intact, free of ReS_2 contamination.

The unit-cell parameter was calculated for the single-phase sodalite structure produced by least-squares refinement of 11–19 powder lines; the values range from 9.071 to 9.118 Å (Table 1). The principal factor causing variation in the *a* parameter of the sodalite is the nature of the cage anion, because SO_4^{2-} is much more bulky than OH^-, S^{2-} and Cl^- (and H_2O). The effect of sulfate on unit-cell size is well shown by the progressive increase in the *a* parameter for the ideal end-members listed above: from 8.882 Å for sodalite (X = Cl) and lazurite (X = S), to 9.084 Å for nosean (X_2 = SO_4•H_2O) and 9.116 Å for haüyne (X = SO_4). The separate and different-sized cages for SO_4^{2-} and S^{2-} in lazurite result in positional disorder of the framework oxygen atoms (Hassan *et al*. 1985). Clearly, on the basis of values of the *a* parameter, the sodalite cage of the present single-phase experimental products is dominated by sulfate. The colorless sodalite phase of experiments without reduced sulfur, and in particular with sulfur added as $CaSO_4$•$2H_2O$, appears to be haüyne. The colored products reported in Table 1 are predominantly lazurite, as presently defined, with cage anions dominated by sulfate. However, as explained below, all of our "lazurite" products coexist in intergrowth relationship with variable amounts of a colorless, low-sulfur sodalite phase that is not differentiated from the colored sodalite in the powder X-ray-diffraction analysis.

Colored crystalline products are associated exclusively with experiments yielding a sodalite-structure phase and containing sulfur in more than one oxidation state (*i.e*., S^{6+} + reduced S). Experiments with either $CaSO_4$ or $CaSO_4$•$2H_2O$ alone resulted in colorless crystalline products. The pale blue sodalite of the hydrothermal-pressure experiment LZ10 (Table 1), which appears to contradict this conclusion, may represent incipient reduction of sulfate by H_2, which has a perceptible leak-rate through gold capsules in long-duration experiments. In addition, all vitreous products from piston–cylinder experiments of this study and sealed evacuated silica-glass tube experiments of the accompanying paper (Fleet *et al*. 2005) are colorless, regardless of starting composition. Colored lazurite resulted from experiments with $CaSO_4$ + CaS, and the blue color faded with decrease in the proportion of sulfate to sulfide. LZ07 is typical of the hydrothermal-pressure products. Pigmentation was limited to 1–5 μm diameter, ill-defined, wispy grains of blue lazurite within a matrix of colorless sodalite of low S content. Sodalite-phase products were much better crystallized in the higher-temperature (1100–1200°C) piston–cylinder experiments, and royal and azure blue colors resulted from experiments with added Re foil. The most successful experiment was LZ67 (Table 1, Fig. 1). Although the product appeared to be homogeneously colored single-phase lazurite on superficial examination (Fig. 1), optical microscopy and EMPA revealed a complex two-phase polycrystalline assemblage (Fig. 2) of equant grains displaying cubic crystal forms and consisting of royal blue lazurite up to 10 μm in size in a generally colorless matrix. In electron back-scattering images, the grain margin of the lazurite crystals was found to be *slightly* darker than the grain core (the core-to-margin contrast is exaggerated in Fig. 2). In the interior of the charge, the matrix is present only as a selvage to lazurite crystals but increases in proportion outward and is most abundant against the Re foil liner. The colorless to very pale green matrix is more dominant near the Re foil in other piston–cylinder experiments, particularly LZ62. The control of proportion of $CaSO_4$ to CaS on color development was not investigated systematically, but the optimum ratio seems to be near 3:1.

Two experiments on the direct synthesis of "ultramarine" of ideal composition $Na_6Al_6Si_6O_{24}$•$2NaS_3$ (which corresponds to the maximum complement of the S_3^- radical anions; see Gobeltz-Hautecoeur *et al*. 2002) were only partially successful (Table 1). High-pressure reaction at 850°C yielded the complex assemblage nepheline + "ultramarine" + ReS_2. The product is blue, but the color is much less vibrant than the royal blue lazurite of experiment LZ67.

Chemical composition of lazurite

All of the present compositional data for synthetic sodalite and natural lazurite are on a H_2O-free basis, and have been reduced to formulae assuming that (Al + Si) equals 12 cations *pfu*, sulfur is exclusively in the cage anion role, and reduced sulfur is sulfide (S^{2-}). The EPMA data for the royal blue crystals from experiment LZ67 resulted in a formula close to $Na_6Ca_2Al_6Si_6O_{24}(SO_4,S)_2$ (Table 2). Aluminum is actually slightly in excess of Si, with the formula ratio Al:Si being about 1.1 to 1.2 (Fig. 3). This Al-for-Si substitution is charge-compensated by an apparent excess of cage cations. Based on the oxide total, the proportion of sulfide sulfur in the royal blue LZ67 product is estimated to be about 10% of the total sulfur *pfu*. Although this estimate is at best semiquantitative, it is clear that, in agreement with the high value of the *a* unit-cell parameter for this sample, S^{6+} is by far the dominant oxidation state. Also, the net ionic charge, calculated for an anhydrous formula from [(total cation charge) – (total anion charge)], is close to zero (Fig. 4). The EPMA spots for LZ67 were located in the center of larger crystals of lazurite to avoid contamination from the colorless matrix (Fig. 2). Because the crystal margins are very narrow, we were unable to specifically test for a core-to-margin compositional gradient. The individual probe-points do reveal a range in solid solution, but this probably reflects compositional change both from core to margin and across the capsule from the interior toward the Re foil.

The EPMA composition of the colorless matrix of LZ67 results in a Si-excess, S-poor sodalite formula (Figs. 3, 4) with Al/Si values near 0.8. Sodium is low (about 4.5 cations *pfu*), but the deficiency of Al and Na together do not compensate for the low cage-anion

charge because the net anhydrous ionic charge is between 3+ and 4+. The three composition points in Figure 3 were taken from the broader areas of colorless matrix (3–5 μm wide), but there remains the potential for contamination from the surrounding royal blue margins. However, the data for LZ67 are consistent with the composition trend of colorless matrix from LZ62 and LZ66 (Figs. 3, 4, Table 1). These two experiments (LZ62 and LZ66) yielded a higher proportion of matrix, which was therefore more readily analyzed; most of the spot analyses are for wide areas of colorless matrix from the outer zone of the charge, near the Re foil liner. The individual composition points define a trend of Si enrichment and S and Na depletion, consistent with the substitutions:

$$\square_A + Si = Na + Al \quad (3)$$

where $\square$ represents a cavity-cation vacancy, and

$$O = (SO_4,S) \quad (4)$$

and a formula of $Na_{5.5-x}Ca_{2.25}Al_{6-x}Si_{6+x}O_{24}(SO_4,S)_{1-y}O_{1+y}$, with $0 < x < 1.5$, $y = (2/3)x$. The limiting composition (from experiment LZ66) corresponds to about $Na_4Ca_{2.25}Al_{4.5}Si_{7.5}O_{24}O_2$. This reconstruction assumes that the colorless phase from these high-pressure experiments has the sodalite structure and that the sulfur cage-anions are replaced by oxygen, in the anhydrous system. Hydroxyl formed from the diffusion of hydrogen through the platinum capsule wall is also a possible cage-anion substituent, but note that the substitution of Al by Si will reduce the size of the sodalite framework and, thus, promote accommodation of the less bulky oxygen anion. Regardless of these speculative details, the composition plots for the colorless matrix do not support compositional continuity with the predominant royal blue phase. These two synthetic phases have distinct compositions, and their composition fields are separated by a well-defined miscibility gap (Fig. 3). A few EPMA spots for experiment LZ07 (Table 1) appeared to extend the composition series of the colorless matrix to about Al/Si ≈ 0.5 under hydrothermal-pressure conditions. Systematic analysis of the products of the hydrothermal-pressure experiments was not attempted owing to the intimate intergrowth relationship of the sodalite phases.

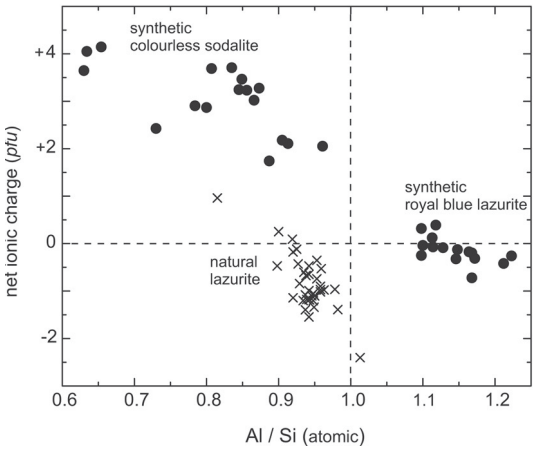

FIG. 4. Variation of net ionic charge [*i.e.*, (total cation charge) – (total anion charge) for anhydrous, cage-oxygen-free formula] with framework composition for blue lazurite and colorless sodalite matrix from high-pressure experiments (small solid circles) and natural lazurite (crosses; computed mainly from compositions in Hogarth & Griffin 1976).

The present EPMA data for the Afghanistan lazurite (2746) are broadly consistent with the microchemical analysis in Taylor (1967), except for higher MgO and CaO and lower Na_2O in the latter, and result in similar contents of S^{6+} and S^{2-} (Table 2). Our EPMA data for the Baffin Island sample (1343) are in good agreement with Hogarth & Griffin (1976) (Table 2) and the blue lazurite of Cade (2003). In marked contrast to the present synthetic royal blue lazurite (LZ67), natural lazurite tends to have an excess of Si in tetrahedral sites, with Al/Si generally being in the range 0.92 to 0.98 (*e.g.*, Fig. 4). Only one of the more than forty compositions of lazurite in Hogarth & Griffin (1976) has Al in excess of Si. This sample is from Slyudyanka, Russia (Voskoboinikova 1938), which in overall composition is very similar to LZ67. In addition, lazurite from Baffin Island tends to have Na ≈ 7, K ≈ 0, Ca ≈ 2, and $(SO_4,S) < 2$ *pfu*. Hogarth & Griffin (1976) found no significant difference in composition between intergrown light blue and dark blue lazurite and color-zoned lazurite from Baffin Island, but they did note a tendency for pale-to-medium blue interstitial grains to have a higher Cl content compared with adjacent dark blue inclusions within diopside. On the other hand, Cade (2003) observed a correlation between the composition of lazurite and its color, which varies from a bleached light green to blue indigo. The formula ratio (Si + Na)/(Al + Ca) increases linearly from the ideal value of 1.5 for light green lazurite to 1.86 for blue indigo lazurite. This trend is opposite to that suggested by compositions for the light matrix sodalite phase and blue lazurite from the piston–cylinder experiments (Fig. 3).

Hogarth & Griffin (1976) reported a drop in counting rate for Na, Cl and S under a stationary electron-beam during EPMA of lazurite, which they compensated for by using a defocused beam and traversing the sample stage. We observed a noticeable drop in counts for Na with continued exposure to the electron beam for the two samples of natural lazurite and, therefore, reduced the counting time and switched off the background measurement for this element after the first spot-analysis. Interestingly, the synthetic royal blue lazurite (LZ67) is stable under the electron beam, as are grains of the colorless S-poor sodalite phase. Evidently the

Na^+ cations are more firmly bound to the framework oxygen atoms in the synthetic lazurite; this effect is possibly a consequence of the Al-for-Si substitution and the reduced contribution of valence by the tetrahedral cations.

Chemical spectroscopy

The S *K*-edge XANES spectra of the samples of synthetic lazurite and haüyne and natural lazurite and scapolite (Figs. 5 to 7, Table 3) are collectively more complex than the spectra of the S-bearing glasses discussed in the accompanying paper (Fleet *et al*. 2005), and have the potential for being a composite of absorption edges of several oxidation states of sulfur. The reference compounds in Table 3 encompass the expected range in chemical state of sulfur. Sulfate and sulfite are indicated by sharp peaks at about 2482 (peak **4** in Fig. 5) and 2478 eV, respectively. The thiosulfate species is characterized by two sharp peaks, at 2471.3 (peak **1** in Fig. 6a) and about 2480 eV (peak **3** in Fig. 6a), representing the edges for S^{2-} bonded to Na and S^{6+} bonded to oxygen and the thio sulfur atom, respectively, and a distinctive overall XANES profile. The XANES spectrum of $NaHS•xH_2O$ (Fig. 6b) appears to confirm the assignment of peak **1** (at 2471.5 eV) to S^{2-} bonded to Na. Sulfide bonded to Ca in the sodalite cavity should result in a broad edge-peak at 2474–2475 eV (*e.g*., peak **2** in Fig. 6b). Unfortunately, there is ambiguity in the assignment of S *K*-edge XANES features to polysulfides and polysulfide radical anions, because the edge peaks for S^{2-} bonded to Na at 2471.3–2471.5 eV, sulfarsenide (AsS^{2-}) bonded to Fe at 2471.2 eV, disulfide (S_2^{2-}) bonded to Fe at 2471.5 eV (Table 6 of Fleet *et al*. 2005), and native sulfur at 2472.0 eV all crowd into the 2471–2472 eV spectral range. We attempted to resolve this ambiguity using S *L*-edge XANES measurements with the grasshopper beamline (*e.g*., Kasrai *et al*. 1996a, Farrell *et al*. 2002), but found that the signal strength for the sodalite phases is too weak for a meaningful interpretation.

The S *K*-edge XANES spectrum of synthetic haüyne (experiment LZ11) has a single sharp peak at 2481.7 eV (peak **4** in Fig. 5b) consistent with sulfate bonded to Ca and Na: the edge features for gypsum and Na_2SO_4 are at 2481.8 and 2481.9 eV, respectively. This XANES result for LZ11 is in agreement with the starting composition, unit-cell parameter and EPMA (not presently reported), which are all consistent with a composition close to ideal haüyne [$Na_6Ca_2Al_6Si_6O_{24}(SO_4)_2$]. The XANES spectrum of LZ11 is, in fact, strikingly similar to that of gypsum (Fig. 1 of Fleet *et al*. 2005); as noted in the accompanying paper, this is because contributions to the extended XANES spectrum are dominantly from the first coordination sphere, and the geometry of the strongly bonded SO_4 tetrahedron is essentially unchanged from gypsum, anhydrite and haüyne. Importantly, note that the background on the low-energy side of the edge peak is featureless. Any absorption in this region would indicate the presence of sulfur in an intermediate or reduced oxidation state.

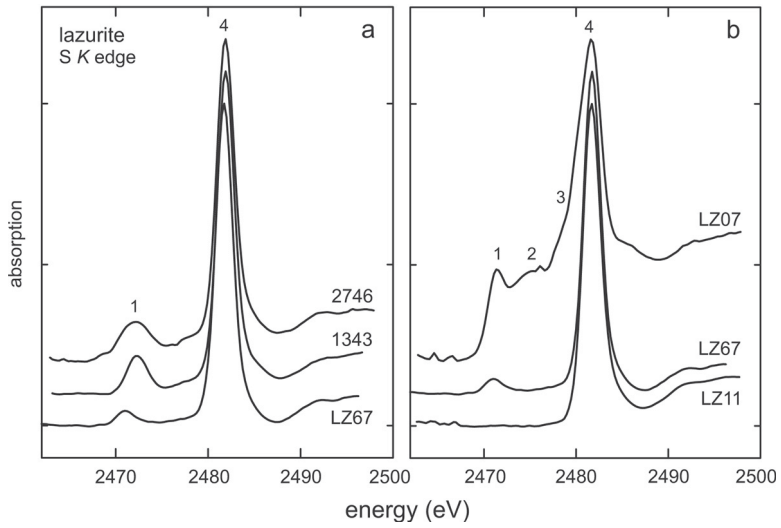

FIG. 5. Sulfur *K*-edge XANES spectra for lazurite from Afghanistan (2746), Baffin Island (1343) and high- (LZ67) and hydrothermal-pressure (LZ07) synthesis: note that synthetic haüyne (LZ11) contains a single edge-peak for sulfate; other reference compounds are listed in Table 3; spectra recorded in TEY mode.

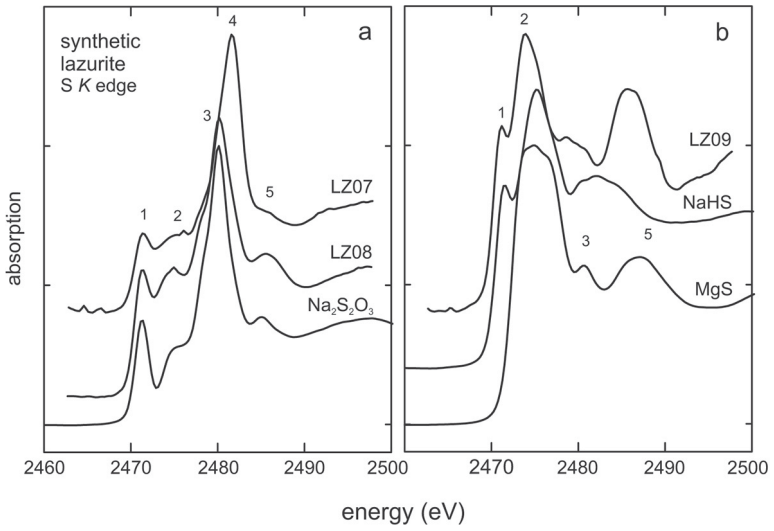

FIG. 6. Sulfur *K*-edge XANES spectra for hydrothermal-pressure experiments employing CaS + $CaSO_4$ redox (LZ07, LZ08) and with CaS as the only sulfur species in the starting composition (LZ09): spectra recorded in TEY mode.

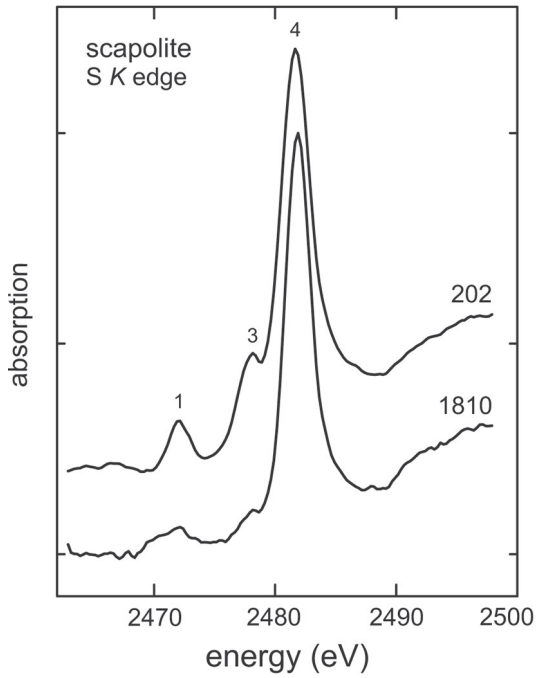

FIG. 7. Sulfur *K*-edge XANES spectra for scapolite from Tsarasaotra, Madagascar (202; 0.36 wt% S) and Craigmont, Ontario (1810; 0.44 wt% S): spectra recorded in TEY mode.

The S *K*-edge XANES spectrum of LZ08 is dominated by thiosulfate (Fig. 6a). The starting composition of experiment LZ08 is consistent with an auto-redox reaction of the type:

$$Na_2O + CaS + CaSO_4 \bullet 2H_2O \rightarrow Na_2S_2O_3 + 2CaO + 2H_2O \quad (5)$$

Sodium thiosulfate disproportionates at 450°C, but it is possible that $(Ca,Na_2)S_2O_3$ is stabilized up to ~800°C by the sodalite framework. As an alternative, the thiosulfate complex may have formed during quenching. The XANES spectrum of experiment LZ07 (with sulfur added as CaS + $CaSO_4$; Table 1) is dominated by sulfate (peak **4** in Fig. 6a) with a subordinate amount of thiosulfate. In contrast, the S *K*-edge peaks for experiment LZ09 (with sulfur added only as CaS) are consistent with sulfide bonded to Na (peak **1** at 2471.2 eV in Fig. 6b) and Ca (peak **2** at 2474.0 eV in Fig. 6b). Halite-structure MgS (synthetic niningerite) is used as a reference compound here because the S *K* edge of the isostructural compound CaS (oldhamite) is complicated by a strong multiple scattering feature (peak **b** in Fig. 3 of Fleet *et al.* 2005) related to the extended halite structure. Even so, the edge feature of the MgS spectrum is anomalously broadened as well, by overlap with the equivalent multiple-scattering feature, compared with the peak width for S bonded to Ca in sodalite. The relatively narrow width of peak **1** in the spectrum for LZ09 (Fig. 6b), compared with the NaHS

reference compound, is no doubt related to the rigid aluminosilicate framework of the sodalite phase.

Sample LZ67 is the only piston–cylinder product investigated by S *K*-edge XANES spectroscopy. The products of the other high-pressure experiments yielding royal blue lazurite were contaminated by ReS_2. The S *K*-edge XANES spectrum of LZ67 in Figure 5 was obtained from a polycrystalline plate cleaved from the compacted plug of product lazurite and is free of grains of ReS_2. The spectrum is dominated by sulfate (peak **4** at 2481.7 eV) with minor reduced sulfur (peak **1** at 2471.0 eV). Based on the fitted peak areas, reduced sulfur amounts to only about 4.4% of total sulfur. This is appreciably less than that estimated from the EPMA analysis (10.8%; Table 2), but note that the oxide total method is at best only semiquantitative. The sulfate component of the XANES spectrum is in excellent agreement with the S *K*-edge XANES spectra of LZ11 (Fig. 5b) and gypsum (Fig. 1 of Fleet *et al*. 2005): sulfate is thus bonded to both Ca and Na. However, the reduced sulfur species is clearly bonded only to Na (Fig. 5b, Table 3).

The S *K*-edge XANES spectra of lazurite from Afghanistan (2746) and Baffin Island (1343) are similar to each other and to that of LZ67 (Fig. 5a), being dominated by the sulfate edge with subordinate reduced sulfur. Compared with LZ67, the reduced sulfur peaks are shifted to slightly higher energy (2472.1 and 2472.3 eV, respectively), possibly indicating polysulfide rather than sulfide. Also, the reduced sulfur region for the Afghanistan sample is broader and has a weak satellite peak at about 2469 eV. From peak areas, reduced sulfur amounts to 14.8 and 11.4% for the Afghanistan and Baffin Island samples of lazurite, respectively; again, these values are considerably lower than the amounts estimated from the oxide totals (41.4 and 29.5%, respectively; Table 2). Note, however, that the estimates from oxide totals are qualitatively correct, with the amount of reduced sulfur corresponding to 16.9% for 2746 and 12.0% for 1343 if normalized to 4.4% for LZ67. The XANES spectrum of the Baffin Island sample is essentially the same as that for the sample of blue lazurite from Baffin Island in Cade (2003): she also found that a sample of the bleached green lazurite had only a weak peak due to reduced sulfur. The S *K*-edge XANES spectra of the two scapolite samples (Fig. 7, Table 3) are included for comparison. They are dominated by sulfate, as expected. The spectrum of scapolite 202 also indicates very minor amounts of sulfite and reduced sulfur, but these features are not evident in the corresponding FY spectrum and in other TEY spectra of this specimen and, therefore, may be artefacts of the sample preparation or of the measurement itself.

TABLE 3. POSITION OF FEATURES IN S *K*-EDGE XANES SPECTRA (eV)[1]

	Reduced S			Oxidized S	
Reference compounds					
$NaHS{\bullet}xH_2O$	2471.5	2475.3	-	-	-
Native S	2472.0	-	-	-	-
CaS	-	2474.1	2477.3	-	-
LZ51[2]	-	2474.9	-	-	-
$Na_2S_2O_3$	2471.3	-	-	2480.1	-
Na_2SO_3	-	-	2477.7	-	-
$Ca_2SO_4{\bullet}2H_2O$	-	-	-	-	2481.8
Experimental products					
LZ07	2471.4	~2475.3	-	-	2481.6
LZ08	2471.4	2474.7	-	2480.2	-
LZ09	2471.2	2474.0	-	-	-
LZ11	-	-	-	-	2481.7
LZ67	2471.0	-	-	-	2481.7
Natural lazurite					
2746	2472.1	-	-	-	2481.9
1343	2472.3	-	-	-	2481.9
Scapolite					
202	2472.1	-	2478.1	-	2481.7
1810	~2471.9	-	-	-	2481.9

[1] TEY (total electron yield) measurements; note that data in Table 6 of accompanying paper (Fleet *et al.* 2005) are from FY (fluorescence yield) spectra.
[2] CaS in Na-aluminosilicate glass.

X-ray photoelectron spectroscopy measures the binding energy (BE) of core electrons from the relationship:

$$KE = h\nu - BE - \phi \quad (6)$$

where KE is the kinetic energy of the emitted photoelectrons, $h\nu$ is the energy of the incident photons (1487 eV for Al$K\alpha$ X-radiation; h is Planck's constant, and ν is frequency), and ϕ is the spectrometer work-function. The binding energy is modulated by the chemical state and stereochemical environment of the atoms probed: selected reference-values for S $2p_{3/2}$ electrons are given in Table 4. Using an Al$K\alpha$ source, S 2*p* photoelectrons usually traverse approximately 15 monolayers of the sample before attenuation. Thus, 90–95% of the S 2*p* signal recorded by the XPS spectrometer originates from the interior (bulk) of the sample, and 5–10% is from the sample's surface. The S 2*p* binding energy increases by up to 7 eV from sulfide to sulfate (Table 4). Of immediate interest for this study is the fact that XPS offers the potential for resolving the separate contributions from sulfide (S^{2-}), disulfide (S_2^{2-}), polysulfide (S_n^-) and native sulfur (*e.g.*, Smart *et al*. 1999). However, our list of reference binding-energies does not include values for reduced sulfur bound to Ca: crystalline CaS was too unstable under the conditions of analysis to give meaningful XPS results.

The XPS results for the lazurite and "ultramarine" synthesized at high pressure and natural lazurite from Afghanistan and Baffin Island are summarized in Table 5 and Figure 8. The S $2p_{3/2}$ peak positions are those of the fitted spectra, except for the spectrum of

the crushed grain sample of LZ67 [LZ67(a) in Table 5], for which we have applied an arbitrary shift of –0.6 eV to correct for charging. All other S $2p_{3/2}$ peak positions are reproducible to ±0.1 eV. For all three samples of synthetic lazurite analyzed as crushed grains, interference from admixed ReS_2 was significant in the 161.5 to 162.5 eV spectral region, resulting in a composite envelope that was fitted to two S $2p_{3/2}$ peaks centered near 161.7 and 162.3 eV. The spectra of the other samples contain a single S $2p_{3/2}$ peak at about 162.0 eV, assigned to sulfide (S^{2-}) bonded to Na (Table 5). In confirmation of this interpretation, powder X-ray-diffraction patterns revealed that the amount of ReS_2 in the crushed grains is major in LZ65, moderate in LZ66, and minor in LZ67: the relative S 2*p* peak areas for reduced sulfur in the XPS spectra are 64% for LZ65, 44% for LZ66 and 21% for LZ67 (Table 5). Taking the effect of ReS_2 contamination into account, it is evident that sulfate is the dominant form of sulfur in all samples investigated by XPS. The contribution of sulfide (S^{2-}) bonded to Na also is very significant. In addition, the synthetic samples of lazurite LZ65 and LZ67 and "ultramarine" BU02 contain a minor amount of sulfite, and the two natural samples of lazurite may contain a minor amount of native sulfur, although this latter assignment is tentative (Fig. 8). Both the sulfite and native sulfur are possibly products of auto-redox reactions at the sample surface (or near surface) during either sample preparation or XPS measurements (*e.g.*, Smart *et al.* 1999). As noted in Smart *et al.* (1999), elemental sulfur is expected to evaporate in the ultra-high XPS vacuum, unless the surface is maintained at <200 K. Therefore, the presently resolved native sulfur would have to be a cage constituent of the bulk structure. Importantly, the XPS spectra do not show evidence of polysulfides. Thus if polysulfides are present they occur below the level of detection in these materials, which is conservatively <1% of total sulfur. The S 2*p* XPS spectra of lazurite from Afghanistan (Fig. 8) and Baffin Island are remarkably similar to each other and distinct from the spectra of the synthetic samples (which are represented in Figure 8 by the XPS spectrum for the plate sample of LZ67).

There is overall agreement between the S *K*-edge XANES and S 2*p* XPS studies of the same sample (*i.e.*, for the synthetic lazurite LZ67 and natural samples of lazurite from Afghanistan and Baffin Island). Both methods show that sulfate is the dominant form of sulfur, in agreement with the values of unit-cell parameter (*a*) and oxide totals, and that there are also significant amounts of reduced sulfur present. The XANES spectra indicate that the latter component is associated with Na (rather than Na and Ca) in the sodalite cages (Fig. 5). There is a significant shift in the position of the reduced sulfur peak in the XANES spectra from synthetic lazurite to natural lazurite, which may be related to the different composition of their framework constituents, Al excess in LZ67 and Si excess in the Afghanistan and Baffin Island lazurite. In addition, the S 2*p* XPS spectra reveal that the reduced sulfur species is exclusively sulfide in the synthetic lazurite and "ultra-

TABLE 4. REFERENCE SULFUR 2*p* XPS BINDING ENERGIES (BE)

Compound	BE	Reference[2]	Compound	BE	Reference[2]
Fe_7S_8 (pyrrhotite)[1]	161.2	1	$Cu_3(S_4)_3$	163.0	6
			PtS_5	163.2	6
$CuFeS_2$ (chalcopyrite)[1]	161.4	2	native S	164.3	4
				163.6-164.0	1
Cu_5FeS_4 (bornite)[1]	161.5	3	$Na_2S_2O_3$	162.5	4
				168.6	
ZnS	161.7	4	Na_2SO_3	166.6	4
Na_2S	161.9	this study	Na_2SO_4	169.1	4
WS_2	162.8	4	$CaSO_4•2H_2O$	169.0	this study
ReS_2	162.6	this study	$CuSO_4$	169.1	4
FeS_2 (pyrite)[1]	162.7	5			

[1] sample fractured in vacuum.
[2] References: 1 Smart *et al.* (1999), 2 Harmer *et al.* (2004), 3 Harmer *et al.* (2005), 4 Briggs & Seah (1990), 5 Harmer & Nesbitt (2004), 6 Termes *et al.* (1987).

TABLE 5. SULFUR 2*p* XPS ANALYSIS OF SYNTHETIC AND NATURAL LAZURITE AND "ULTRAMARINE"[1]

Sample no.	Sulfur host	Position of S $2p_{3/2}$ (eV)	Area of S 2*p* doublet (%)	Peak assignment
LZ65	Synthetic lazurite	161.8[2]	18.1	sulfide(S^{2-})-Na
		162.4[3]	45.7	ReS_2
		166.9	8.6	sulfite
		168.8	27.7	sulfate
LZ66	Synthetic lazurite	161.6[2]	9.5	sulfide(S^{2-})-Na
		162.3[3]	34.0	ReS_2
		169.0	56.5	sulfate
LZ67(a)	Synthetic lazurite	160.7[4]	1.9	–
		162.3[2]	19.2	S^{2-}-Na; ReS_2 (minor)
		167.0	12.2	sulfite
		168.9	66.8	sulfate
LZ67(b)	Synthetic lazurite (plate)	162.1	18.6	sulfide(S^{2-})-Na
		166.9	13.6	sulfite
		168.9	67.7	sulfate
2746	Lazurite (Afghanistan)	162.0	7.8	sulfide(S^{2-})-Na
		164.2	4.0	native sulfur
		169.1	88.2	sulfate
1343	Lazurite (Baffin Island)	161.8	13.1	sulfide(S^{2-})-Na
		164.2	5.4	native sulfur
		168.8	81.5	sulfate
BU02	"Ultramarine"	161.3	3.1	–
		162.0	23.8	sulfide(S^{2-})-Na
		166.9	4.5	sulfite
		169.0	68.5	sulfate

[1] lazurite and "ultramarine" synthesized at high pressure; samples analyzed as crushed polycrystalline grains, except as indicated.
[2] peak position in error due to interference from ReS_2.
[3] peak position in error due to interference from sulfide(S^{2-})-Na.
[4] all peak positions for LZ67(a) have been shifted by –0.6 eV to compensate for charging.

marine" BU02 and sulfide with, perhaps, native sulfur in natural lazurite.

Although XANES and XPS both probe chemical state through excitation of core electrons, spectral differences from one method to the other are expected because XANES reflects both initial and final electron states, whereas only the initial electron states are important in XPS. In addition, XPS is intrinsically more surface-sensitive than XANES, particularly for XANES spectra recorded in the FY mode: maximum depths of sampling are ~15 monolayers for S 2*p* XPS compared with ~700 Å for the TEY mode and several thousand ångströms for the FY mode of S *K*-edge XANES (*e.g.*, Kasrai *et al*. 1996b). We have seen that where sulfide and sulfate species are both present in the bulk sample, there is the potential for auto-redox reactions to take place in the near-surface region probed by XPS.

There is, however, a major discrepancy in the relative proportion of sulfide to sulfate indicated by the two spectroscopic methods, which is presently unresolved. The sulfide component in the synthetic LZ67 lazurite is 4% by XANES and 19% by XPS, whereas in, for example, the Afghanistan lazurite it is 17% by XANES and 8% by XPS. In support of the S *K*-edge XANES method, differences between the two simultaneous (TEY and FY) measurements are attributed to bulk sensitivity and scaling only. In this study, corresponding TEY and FY spectra were essentially identical in respect to size (peak area and width) and position of spectral features. The TEY spectra have smoother profiles and, therefore, are used for presentation purposes in this paper. Note that the preliminary XPS study of "ultramarine" BU02 suggests that it is sulfate-dominant, but this seems inconsistent with the reduced sulfur in the starting composition of this experiment (Table 1).

Color in lazurite and "ultramarine"

This study has revealed important differences and similarities in the chemical compositions and crystal chemistries of synthetic and natural sodalite-group phases, but none of these features appears to be directly related to the characteristic blue color of lazurite and "ultramarine". All of the present samples of synthetic lazurite were found to be inhomogeneous in both color development and composition, appearing as micrometric intergrowths. In high-pressure products, these were seen to represent the two-phase assemblage (blue, S-rich lazurite + colorless, S-poor sodalite). Color development may also be uneven in the mineral. For example, Hogarth & Griffin (1976) reported dark and light blue lazurite from Baffin Island coexisting as a "perthitic" composite. Natural lazurite differs markedly from its synthetic equivalent in chemical composition (Table 2, Figs. 3, 4), and S *K*-edge XANES (Fig. 5) and S $2p_{3/2}$ XPS spectra (Fig. 8, Table 5), but these differences appear to have little bearing on color development. For example, lazurite from Baffin Island is pale to mid-blue, whereas that from Afghanistan is deep royal blue, and the synthetic lazurite LZ67 also is royal blue (Fig. 1). Hogarth & Griffin (1976) suggested that dark blue varieties of lazurite contain a higher proportion of sulfide than the light blue varieties. This correlation is clearly contradicted by our experimental products (Table 1). Although both sulfide and sulfate must be present, color intensity appears to actually decrease with increase in proportion of sulfide.

As is well known from the many studies on the synthesis of "ultramarine", color development in these pigments is associated with synthesis and annealing of the aluminosilicate sodalite structure in the presence of a reducing agent, followed by further annealing at higher temperature (to 750–800°C) in an oxidizing atmosphere, although the oxidizing step may be unne-

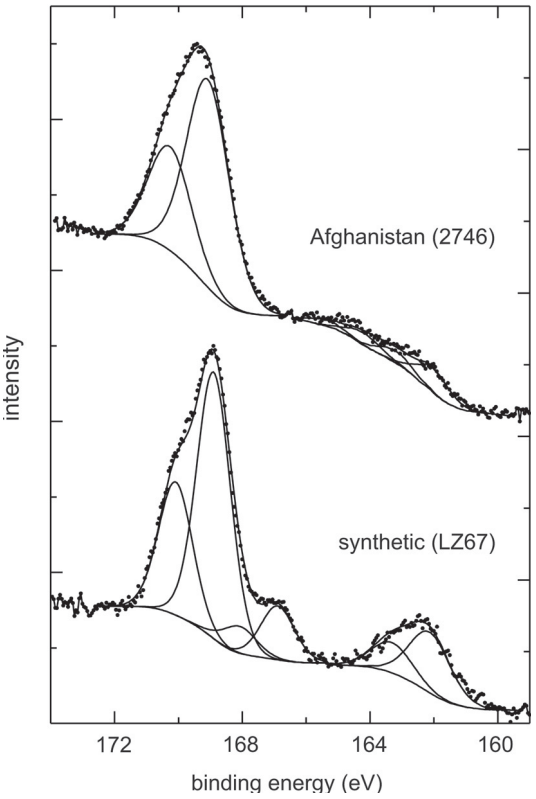

FIG. 8. Sulfur 2*p* XPS spectra for lazurite from Afghanistan (2746), showing peaks due to sulfate, sulfide bonded to Na and, possibly, elemental sulfur, and synthetic lazurite LZ67 (Table 1), showing peaks due to sulfate, sulfide bonded to Na and sulfite. Small full circles are experimental measurements, and curves are: (i) calculated Shirley background, (ii) fitted Gaussian–Lorentzian peaks for S $2p_{3/2}$ and S $2p_{1/2}$ (in 2:1 ratio), and (iii) resulting fitted envelope: note that both samples of lazurite are royal blue; see Table 4 for positions of reference peaks.

cessary if annealing in a reducing atmosphere is continued up to 800°C (Gobeltz *et al*. 1998b). Furthermore, lazurite usually occurs with pyrite in nature, suggesting prolonged metamorphic annealing under reducing conditions. In the present experiments, reduction of sulfate occurred by reaction with sulfide *via* auto-redox reactions like (1) and (5) above and by reaction with Re metal foil [reaction (2)]. The texture of the LZ67 intergrowth (Fig. 2) is also consistent with annealing during reduction, resulting in progressive loss of sulfur from the silicates to form ReS_2 and reduction of sulfate in blue lazurite. More generally, the present experiments suggest that poorly crystalline sodalite (or "proto-sodalite") forms quickly on heating the starting materials, and the blue color develops progressively on further annealing either by diffusion of the chromophore(s) into the sodalite cages (Gobeltz *et al*. 1998b) or production of the polysulfide chromophore(s) from reduction of sulfate or reaction between sulfate and sulfide in adjacent cages. In experiments with no reduced sulfur in the starting composition, for example, the "proto-sodalite" would be haüyne-like.

Unlike "ultramarine", synthetic and natural lazurite do not appear to contain measurable amounts of polysulfides and, in particular, of the radical anions S_3^- and S_2^-, which have been identified as the important chromophores (Clark & Franks 1975, Clark *et al*. 1983, Gobeltz *et al*. 1998a, b, Reinen & Lindner 1999, Gobeltz-Hautecoeur *et al*. 2002). Furthermore, the temperature of annealing in the piston–cylinder experiments (1200°C; Table 1) would seem to be too high for polysulfide formation, even where bound in a silicate framework. At the same time, very minor quantities of impurities or defects create color in crystals and glasses. In comparison, if S_3^- is indeed the blue chromophore in "ultramarine" and occupies up to one-half of the sodalite cages (Gobeltz-Hautecoeur *et al*. 2002), it must be very inefficient at absorbing light in the region above 21,500 cm^{-1}. Perhaps the strength of coupling of the radical anion with the sodalite framework or cage cations is an important factor here. Identification of the chromophore (or pigmentation reaction) in lazurite will be difficult, but in this study, we have made significant steps to eliminate a number of possible factors bearing on this problem. One obvious area for further research is XANES and XPS study of sulfide "ultramarine".

Acknowledgements

We thank Shannon Farrell and a second, anonymous reviewer for helpful comments, Menghua Liu and Andrei Barkov for EPMA data, Jisuo Jin for assistance with photography, Astrid Jürgensen and Kim Tan, Canadian Synchrotron Radiation Facility, and staff of the Synchrotron Radiation Centre (SRC), University of Wisconsin-Madison, for their technical assistance, and the National Science Foundation (NSF) for support of the SRC under the grant DMR–0084402. This work was supported by the Natural Sciences and Engineering Research Council of Canada.

References

Barth, T.F.W. (1932): The structure of the minerals of the sodalite family. *Z. Kristallogr.* **83**, 405-414.

Berg, R.W., Bjerrum, N.J., Papatheodorou, G.N. & Von Winbush, S. (1980): Resonance Raman spectra of S_3^- in molten salts. *Inorg. Nucl. Chem. Lett.* **16**, 201-204.

Bohlen, S.R. (1984): Equilibria for precise pressure calibration and a frictionless furnace assembly for the piston–cylinder apparatus. *Neues Jahrb. Mineral., Monatsh.*, 404-412.

_____ & Boettcher, A.L. (1982): The quartz → coesite transformation: a precise determination and the effects of other components. *J. Geophys. Res.* **87**, 7073-7078.

Briggs, D. & Seah, M.P., eds. (1990): *Practical Surface Analysis*. 1. *Auger and X-ray Photoelectron Spectroscopy* (2nd ed.). John Wiley & Sons, Chichester, U.K.

Cade, A.M. (2003): *Coloration of Lazurite from Baffin Island, Nunavut*. M.Sc. thesis, Univ. Western Ontario, London, Ontario.

Clark, R.J.H., Dines, T.J. & Kurmoo, M. (1983): On the nature of the sulphur chromophores in ultramarine blue, green, violet, and pink and of the selenium chromophore in ultramarine selenium: characterization of radical anions by electronic and resonance Raman spectroscopy and the determination of their excited-state geometries. *Inorg. Chem.* **22**, 2766-2772.

_____ & Franks, M.L. (1975): The resonance Raman spectrum of ultramarine blue. *Chem. Phys. Lett.* **34**, 69-72.

Farrell, S.P., Fleet, M.E., Stekhin, I.E., Kravtsova, A., Soldatov, A.V. & Liu, Xiaoyang (2002): Evolution of local electronic structure in alabandite and niningerite solid solutions [(Mn,Fe)S, (Mg,Mn)S, (Mg,Fe)S] using sulfur *K*- and *L*-edge XANES spectroscopy. *Am. Mineral.* **87**, 1321-1332.

Fleet, M.E. (1989): Structures of sodium alumino-germanate sodalites [$Na_8(Al_6Ge_6O_{24})A_2$, *A* = Cl, Br, I]. *Acta Crystallogr.* **C45**, 843-847.

_____, Liu, Xiaoyang, Harmer, S.L. & King, P.L. (2005): Sulfur *K*-edge XANES spectroscopy: chemical state and content of sulfur in silicate glasses. *Can. Mineral.* **43**, 1605-1618.

Gaines, R.V., Skinner, H.C.W., Foord, E.E., Mason, B. & Rosenzweig, A. (1997): *Dana's New Mineralogy* (8th ed.). John Wiley & Sons, New York, N.Y.

Gobeltz, N., Demortier, A., Lelieur, J.P. & Duhayon, C. (1998a): Correlation between EPR, Raman and colorimetric characteristics of the blue ultramarine pigments. *J. Chem. Soc., Faraday Trans.* **94**, 677-681.

_____, _____, _____ & _____ (1998b): Encapsulation of the chromophores into the sodalite structure during the synthesis of the blue ultramarine pigment. *J. Chem. Soc., Faraday Trans.* **94**, 2257-2260.

GOBELTZ-HAUTECOEUR, N., DEMORTIER, A., LEDE, B., LELIEUR, J.P. & DUHAYON, C. (2002): Occupancy of the sodalite cages in the blue ultramarine pigments. *Inorg. Chem.* **41**, 2848-2854.

HARMER, S.L. & NESBITT, H.W. (2004): Stabilization of pyrite (FeS_2), marcasite (FeS_2), arsenopyrite (FeAsS) and loellingite ($FeAs_2$) surfaces by polymerization and auto-redox reactions. *Surface Sci.* **564**, 38-52.

_____, PRATT, A.R., NESBITT, H.W. & FLEET, M.E. (2004): Sulfur species at chalcopyrite ($CuFeS_2$) fracture surfaces. *Am. Mineral.* **89**, 1026-1032.

_____, _____, _____ & _____ (2005): Reconstruction of fracture surfaces on bornite. *Can. Mineral.* **43**, 1619-1630.

HASSAN, I. & GRUNDY, H.D. (1984): The crystal structures of sodalite-group minerals. *Acta Crystallogr.* **B40**, 6-13.

_____ & _____ (1989): The structure of nosean, ideally $Na_8[Al_6Si_6O_{24}]SO_4 \bullet H_2O$. *Can. Mineral.* **27**, 165-172.

_____ & _____ (1991): The crystal structure of hauyne at 293 and 153 K. *Can. Mineral.* **29**, 123-130.

_____, PETERSON, R.C. & GRUNDY, H.D. (1985): The structure of lazurite, ideally $Na_6Ca_2(Al_6Si_6O_{24})S_2$, a member of the sodalite group. *Acta Crystallogr.* **C41**, 827-832.

HOGARTH, D.D. & GRIFFIN, W.L. (1976): New data on lazurite. *Lithos* **9**, 39-54.

_____ & _____ (1978): Lapis lazuli from Baffin Island – a Precambrian meta-evaporite. *Lithos* **11**, 37-60.

JAEGER, F.M. (1929): On the constitution and the structure of ultramarine. *Trans. Faraday Soc.* **25**, 320-345.

KASRAI, M., BROWN, J.R., BANCROFT, G.M., YIN, Z. & TAN, K.H. (1996a): Sulphur characterization in coal from X-ray absorption near edge spectroscopy. *Int. J. Coal Geol.* **32**, 107-135.

_____, LENNARD, W.N., BRUNNER, R.W., BANCROFT, G.M., BARDWELL, J.A. & TAN, K.H. (1996b): Sampling depth of total electron and fluorescence measurements in Si L- and K-edge absorption spectroscopy. *Appl. Surface Sci.* **99**, 303-312.

NESBITT, H.W., SCAINI, M., HÖCHST, H., BANCROFT, G.M., SCHAUFUSS, A.G. & SZARGAN, R. (2000): Synchrotron XPS evidence for Fe^{2+}_S and Fe^{3+}_S surface species on pyrite fracture-surfaces, and their 3D electronic states. *Am. Mineral.* **85**, 850-857.

VAN PETEGHEM, J.K.& BURLEY, B.J. (1963): Studies on solid solution between sodalite, nosean and hauyne. *Can. Mineral.* **7**, 808-813.

REINEN, D. & LINDNER, G.-G. (1999): The nature of the chalcogen colour centres in ultramarine-type solids. *Chem. Soc. Rev.* **28**, 75-84.

SHIRLEY, D.A. (1972): High-resolution X-ray photoemission spectrum of the valence bands of gold. *Phys. Rev. B* **5**, 4709-4714.

SMART, R.ST.C., SKINNER, W.M. & GERSON, A.R. (1999): XPS of sulphide mineral surfaces: metal-deficient, polysulphides, defects and elemental sulphur. *Surface Interface Anal.* **28**, 101-105.

STRUNZ, H. (1970): *Mineralogische Tabellen* (5th ed.). Akademische Verlagsgesellschaft, Leipzig, Germany.

TAUSON, V.L. & SAPOZHNIKOV, A.N. (2003): Nature of lazurite coloration. *Zap. Vser. Mineral. Obshchest.* **132**(5), 102-107.

TAYLOR, D. (1967): The sodalite group of minerals. *Contrib. Mineral. Petrol.* **16**, 172-188.

TERMES, S.C., BUCKLEY, A.N. & GILLARD, R.D. (1987): 2*p* electron binding energies for the sulfur atoms in metal polysulfides. *Inorg. Chim. Acta* **126**, 79-82.

TYLISZCAK, T. (1992): *BAN Data Analysis Program*. McMaster University, Hamilton, Ontario.

VOSKOBOINIKOVA, N. (1938): The mineralogy of the Slyudyanka deposits of lazurite. *Zap. Vses. Mineral. Obshchest.* **67**, 601-622 (in Russ.).

Received August 31, 2004, revised manuscript accepted October 5, 2005.